

Research Article

Volume 2 Issue 5 - September 2017
DOI: 10.19080/JOJMS.2017.02.555600

JOJ Material Sci

Copyright © All rights are reserved by Ferkhi

New Cathode Material, $\text{Nd}_{1.90}\text{Sr}_{0.1}\text{Ni}_{0.9}\text{Co}_{0.1}\text{O}_{4\pm\delta}$, for IT-Solid Oxide Fuel Cell



Ferkhi M^{1,2*}, Amira S^{1,2} and Khaled A²

^{1,2}Department of Chemistry, Mohamed Seddik Ben Yahia University, Algeria

²Laboratory of Materials-Environment Interactions Study (LIME), Mohamed Seddik University Ben Yahia, Algeria

Submission: August 22, 2017; **Published:** September 25, 2017

***Corresponding author:** Ferkhi, Department of Chemistry, Faculty of Exact Sciences and Computer Science, Mohamed Seddik Ben Yahia University. BP98 Ouled Aissa Jijel 18000, Algeria, Email: ferkhimosbah1@gmail.com

Abstract

The Oxygen Reduction Reaction (ORR) was studied on $\text{Nd}_{1.9}\text{Sr}_{0.1}\text{Ni}_{0.9}\text{Co}_{0.1}\text{O}_{4\pm\delta}$ nickeltaes as cathode material at high temperature, the citrate method was used for preparing the material. The study of Oxygen Reduction Reaction was carried out in air at various temperatures. Characterization by XRD and SEM were performed to analyze the crystallinity of the material. XPS analysis is used to evaluate the surface state of the material. Electrochemical studies were followed by impedance spectroscopy. The $\text{Nd}_{1.9}\text{Sr}_{0.1}\text{Ni}_{0.9}\text{Co}_{0.1}\text{O}_{4\pm\delta}$ cathode was deposited as a layer on a Gadolina Doped Ceria (GDC). At high temperature, a significant electrocatalytic activity is observed for the studied material that shows a relatively high electrocatalytic activity for O_2 reduction.

At high temperatures, the $\text{Nd}_{1.9}\text{Sr}_{0.1}\text{Ni}_{0.9}\text{Co}_{0.1}\text{O}_{4\pm\delta}$ material has best electrochemical properties, and the value of the activation energy is much lower compared to several materials synthesized and electrochemically characterized which indicates that $\text{Nd}_{1.9}\text{Sr}_{0.1}\text{Ni}_{0.9}\text{Co}_{0.1}\text{O}_{4\pm\delta}$ electrode is a promising cathode material for intermediate-temperature solid oxide fuel cell (IT-SOFC).

Keywords: XPS analysis; MIEC; SOFC; Impedance spectroscopy; Electrocatalyst materials

Introduction

In the second part of this work, increase the life time of solid oxide fuel cell (SOFC) need lower their operating temperature range of 800-1000 °C to 600-800 °C. This results in decreased electrochemical performance of SOFCs [1-5].

To remedy this, the research has been directed toward the development of new cathode materials called mixed conducting (ion and electron) symbolized MIEC. It's a way to locate the reduction reaction of oxygen to the entire material, and significantly reduce the resistance and associated surges. K_2NiF_4 -type materials such as neodymium nickelates Nd_2NiO_4 , meet these criteria [6,7]. A judicious doping with cerium, srtontium in neodym site and by cobalt or copper in nickel site of this new phase further enhances their electrochemical properties. However, it may in some cases lead to the formation of harmful secondary phases to the cathode/electrolyte interface [8,9].

Soori and Skinner have studied $\text{Nd}_{2-x}\text{Ce}_x\text{CuO}_{4+\delta}$ ($0 \leq x \leq 0.2$) cathode interfaced with both GDC ($\text{Ce}0.9\text{Gd}0.1\text{O}1.95$) and LSGM($\text{La}_{0.9}\text{Sr}_{0.1}\text{Ga}_{0.8}\text{Mg}_{0.2}\text{O}_{3\pm\delta}$) electrolytes [10]. The solid solubility limit of Ce in $\text{Nd}_{2-x}\text{Ce}_x\text{CuO}_4$ has been reported to be at $x=0.2$ [10,11]. At this composition, the lowest value of activation energy ($E_a=0.11\text{eV}$) was measured over a temperature range

of 500 to 700 °C [12]. In K_2NiF_4 -type oxides, perovskite layer, ABO_3 , and rock salt layer, AO, are alternately stacked and they show oxygen excess composition because interstitial oxygen is formed in the rock salt layer [1,13,14].

The $\text{Nd}_2\text{NiO}_{4+\delta}$ and $\text{Nd}_{1.8}\text{Sr}_{0.2}\text{NiO}_{4+\delta}$ materials, in high $\text{P}(\text{O}_2)$ atmosphere, show large oxygen excess composition, while $\text{Nd}_{1.6}\text{Sr}_{0.4}\text{NiO}_{4+\delta}$ show almost stoichiometric oxygen composition.

Space in the rock salt layer decreases as the calculated acceptor concentration, $x+2\delta$, increases. This means that the interstitial oxygen formation is suppressed as the acceptor concentration increases. Similar tendency has been confirmed in oxygen nonstoichiometric behavior of Ni-based K_2NiF_4 -type oxides [15].

$\text{Nd}_2\text{NiO}_{4+\delta}$ has been reported to exhibit promising electrocatalytic activity to oxygen reduction reaction when used as cathode for IT-SOFC [3,6]. The oxygen-diffusion coefficient of $\text{Nd}_2\text{NiO}_{4+\delta}$ is also much higher than that of $\text{La}_2\text{NiO}_{4+\delta}$ [6,16].

The $\text{Nd}_{1.6}\text{Sr}_{0.4}\text{NiO}_4$ electrode gave a polarization resistance of $0.93 \Omega\cdot\text{cm}^2$ at 700 °C in air, which indicates that $\text{Nd}_{2-x}\text{Sr}_x\text{NiO}_4$ electrode is a promising cathode material for intermediate-temperature solid oxide fuel cell (IT-SOFC) [17].

In this work, we were interested to substitutions of small quantities of cobalt, less than 10%, in order to improve the cell performance by limiting the reactivity between cathode materials and electrolyte. $\text{Nd}_{1.90}\text{Sr}_{0.1}\text{Ni}_{0.90}\text{Co}_{0.1}\text{O}_{4\pm\delta}$ powder are prepared, and the electrode were deposited by painting on the electrolyte substrate GDC in both faces. The microstructure and morphology of the samples were analyzed by X-ray diffraction and scanning electron microscopy. The electrochemical performance and a first approach of reaction mechanisms were determined by impedance spectroscopy.

Experimental

The $\text{Nd}_{1.90}\text{Sr}_{0.1}\text{Ni}_{0.90}\text{Co}_{0.1}\text{O}_{4\pm\delta}$ (NSNCO01) cathodes materials were prepared by Pichini process described by Mr. and FERKHI et. al [18,19], leads to the formation of particles with sufficiently fine size in order to increase the active surface of the material. The precursors used in the synthesis are; $\text{Nd}(\text{NO}_3)_{3.6}\text{H}_2\text{O}$ (99.0 % SIGMA- Aldrich), La_2O_3 (Biochem); $\text{Ni}(\text{NO}_3)_{2.6}\text{H}_2\text{O}$ (97,0 % SIGMA- Aldrich); $\text{Co}(\text{NO}_3)_{2.6}\text{H}_2\text{O}$ 98,0 % SIGMA- Aldrich) and $\text{Sr}(\text{NO}_3)_2$ (Biochem). All precursors in a nitrate state are, first, dissolved in distilled water with appropriate amounts but the lanthanum oxide La_2O_3 are dissolved in nitric acid. The mixture of cations is under moderate stirring and a temperature between 75-80 °C.

Then, citric acid ($\text{C}_6\text{H}_8\text{O}_7$) is added in excess acting as a complexing agent. After evaporation of the solvent the solution begins to gel. The gel (viscous mixture) formed is dried at 120 °C and then treating at 174 °C leads to the obtaining of a foam which must be ground and calcined under various temperatures. In this work; electrochemical measurements at high temperatures were carried out on a symmetrical cell $\text{Nd}_{1.90}\text{Sr}_{0.1}\text{Ni}_{0.90}\text{Co}_{0.1}\text{O}_{4\pm\delta}/\text{GDC}/\text{Nd}_{1.90}\text{Sr}_{0.1}\text{Ni}_{0.90}\text{Co}_{0.1}\text{O}_{4\pm\delta}$. Commercial $\text{Ce}_{0.9}\text{Gd}_{0.1}\text{O}_{1.95}$ (GDC) oxide was used as electrolyte. For this, a pellet of diameter 10mm and a thickness of 1.14mm was prepared by uniaxial pressing under a pressure of 8 tons for 7min in a press "Specac". This pellet was then sintered for 2 hours at 1400 °C to achieve a density of 95%. The ink consists of powder drop $\text{Nd}_{1.90}\text{Sr}_{0.1}\text{Ni}_{0.90}\text{Co}_{0.1}\text{O}_{4\pm\delta}$ and ethylene glycol (EG). The powder/EG ratio is one drop to 100mg powder. After mixed, the ink is applied as uniformly as possible on the GDC pellet symmetrically in both sides. Impedance measurements were performed using a configuration with two electrodes, the cell is then placed in a high temperature furnace. A frequency has been used as signal amplitude of 50mV imposed in a frequency range between 10^6Hz and 10^{-2} .

The X-ray diffraction spectra were obtained with a $\text{CuK}\alpha$ radiation (1.5406 Å) of XPERT-PRO type diffractometer. The characteristics of the morphology and microstructure of powders were studied using an electron microscope type JEOL scanning/ EO version 1.07. XPS analyses were performed at the University of Namur, Belgium on a K-Alpha system (ThermoFisher Scientific), equipped with a monochromatic Al-K α source (1486.6eV) and a hemispherical deflector analyzer working at constant pass energy. A 300μm diameter X-ray beam spot was used. Surface charging effects were avoided using an electron

flood gun. The base pressure in the analyzer chamber was $2\times 10^{-8}\text{Pa}$. Survey spectra were recorded with 200eV pass energy and, for high resolution spectra this energy was decreased to 30eV. The Thermo Scientific Advantage software (version 5.943) was used for collecting and processing the spectra. The binding energy shifts were calibrated relative to the adventitious carbon C 1s position fixed at 284.6eV and the BE accuracy was $\pm 0.1\text{eV}$.

Results and Discussion

X-Ray diffraction analysis

Diffraction patterns obtained at room temperature on the neodymium-based nickelates powder and lanthanum calcined at 1000 °C for 4h are shown in Figure 1. These diagrams show that the powders prepared is pure and well crystallized. The peaks were indexed using the JCPDS 21-1274 number and other work [2,17,20,21].

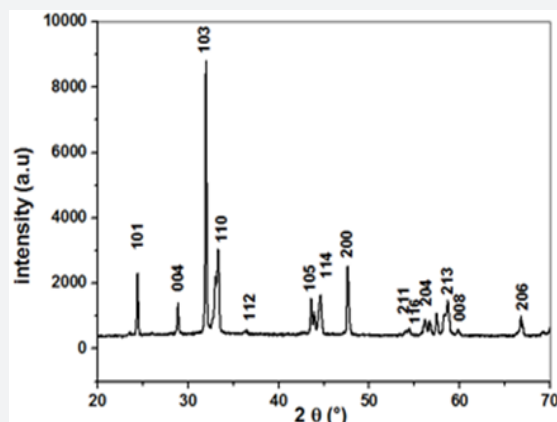


Figure 1: X-Ray Diffraction of $\text{Nd}_{1.9}\text{Sr}_{0.1}\text{Ni}_{0.9}\text{Co}_{0.1}\text{O}_{4\pm\delta}$ patterns sintered at 1000 °C for 4h.

NSNCO01 material was crystallizes in a tetragonal system with a group of spaces I4/mmm (high symmetry system) [17,21]. The refinement of the lattice parameters was performed and the results are; SG (space group): I4/mmm, $a=b=3.8211$, $c=12.3488$, $\alpha=\beta=\gamma 90^\circ$, $V = 180.307 \text{ \AA}^3$ and $D=58.16\text{nm}$.

Morphological analysis

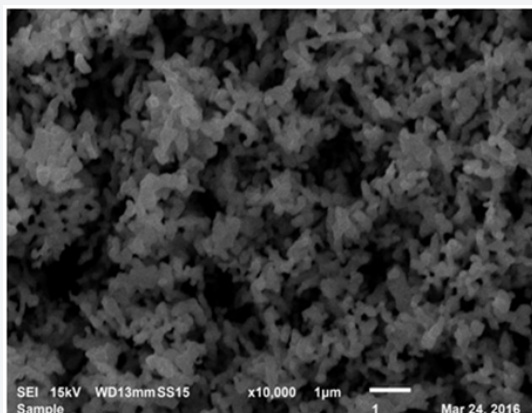


Figure 2: MEB micrographs for NSNCO01 patterns sintered at 1000 °C for 4h with grossissement at 1μm.

From the results of the microstructure (Figure 2), it is observed that the materials are porous which improves its catalytic properties and the same electrocatalytic by increasing the surface area. The grains are forms spheroids with a grain size of about $0.5\mu\text{m}$. The NSNCO01 material is more porous compared to Sr_2MMoO_6 ($\text{M}=\text{Fe}$ and Co) double perovskites materials synthesized and studied previously [22]. Since the specific surface area, which depends on the porosity, double perovskites are of the order of 28 and $17.5\text{m}^2/\text{g}$ respectively. Therefore, the NSNCO01 material can have a larger specific surface area by promoting, there after, the kinetics of the reduction reaction of oxygen.

XPS analysis

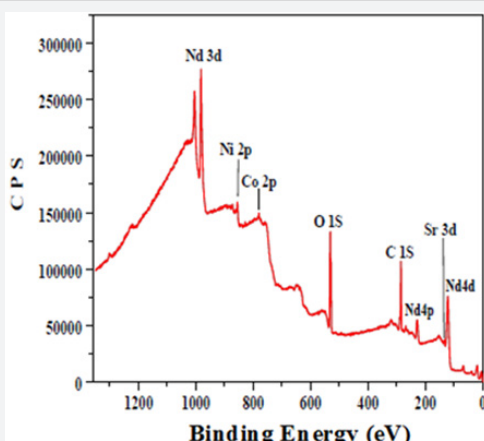


Figure 3: XPS survey of NSNCO01 sample.

The XPS general spectra for neodymium-based material is shown in Figure 3. It is obvious that all the elements that enter into the composition of the materials (including adventitious carbon) are present on the surface. The Figure 4 shows the oxygen peaks (O1s) after deconvolution. Five original peaks were distinguished with different binding energies.

Table 1 : Percentage of the elements in the surface of NSNCO01 material.

Region	O1s	$\text{Nd}_3\text{d}_{5/2}$	$\text{Ni}_{2\text{p}}_{3/2}$	$\text{Sr}_3\text{d}_{5/2}$	$\text{Co}_{2\text{p}}_{3/2}$
Percentage (%)	41.16	10.82	02.30	01.10	01.52

Table 2: Binding Energy of oxygen and percentage of hydroxyl groups at the surface.

Binding Energy (eV)	527.53	528.61	530.17	531.35	533.30	% of oxygen in lattice	OH- in surface
Peak	a	b	c	d	c	47.4	19.58

The concentration ratio between Nd and Ni is a bit larger than the expected; so that we can say that the surfaces of both materials are slightly enriched in Nd. The Sr and Co incorporation does reduce this ratio (enrichment), because we measure that the $(\text{Nd}+\text{Sr})/(\text{Ni}+\text{Co})$ ratio becomes close to the one before doping. From the Nd/Sr and Ni/Co values (16.66 and 1.51 respectively), the Sr and Co amounts on the surface

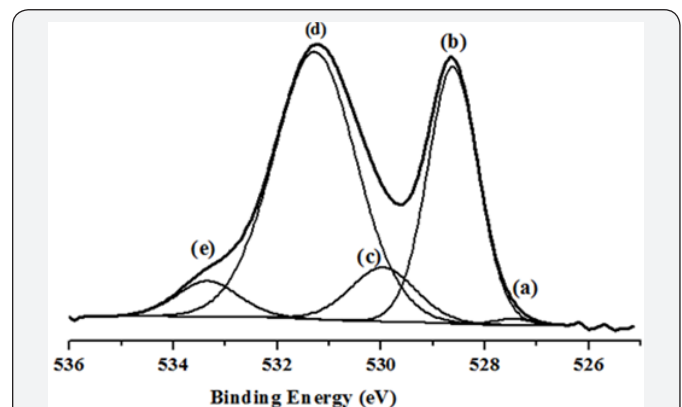


Figure 4: XPS spectra of O 1s regions for NSNCO01 sample.

With regard to the oxygen region, it is well known the presence of various elements of different characters in the mixed metal oxides makes the bond between metal and oxygen not purely ionic. According to the classification established by T. L. Barr [23] we can say that NSNCO01 materials include O-Nd binding of high ionic character and O-Ni bond of normal ionic character. Therefore, the first has a lower binding energy than the second. Sr and Co doping elements in the sample are in very small quantities (Table 1) and belong to the previous two families, respectively. Therefore, their presence does not affect significantly on the energy of O-Nd and O-Ni bonds. Accordingly, the low energy component (a) and (b) at 527.53 and 528.61 eV for NSNCO01 material stands for oxygen anions in neodymium oxides [23,24] and the component (c) at 530.17 eV may denote the oxygen ions in nickel oxides [25]. The component (d) at 531.35 eV can be ascribed to the metal hydroxyl groups because the rare earth oxides are very hygroscopic when exposed to atmospheric conditions [25,26]. The last component (e) at 533.30 eV with highest FWHM presumably arises from adsorbed molecular water (Table 2).

Table 3: ASRs values calculated at 600 °C and 700 °C and activation energy for various materials.

Cathode/Electrolyte	Temperature (°C)	ASR ($\Omega\cdot\text{cm}^2$)	Activation Energy (eV)	Reference
$\text{Nd}_{1.9}\text{Sr}_{0.1}\text{Ni}_{0.9}\text{Co}_{0.1}\text{O}_{4+\Delta}/\text{GDC}$	640	3.40	0.88	This work

are much greater than those of the theoretical stoichiometries. The ratio between the lattice ions and cations at the surface amounts ($\text{Olat} / \Sigma \text{cation}$) show that the surface of NSNCO01 material has a more anionic character. Finally, the XPS analyses tell us that the hydroxyls groups (or oxygen adsorbed in form of OH^-) percentage is 29.64%. This behavior may impact on the electrochemical properties of the materials (Table 3).

$\text{Nd}_{1.8}\text{Sr}_{0.2}\text{Ni}_{0.8}\text{Cu}_{0.2}\text{O}_{4+\delta}/\text{GDC}$	640	2.94	1.39	[28]
$\text{Nd}_{1.8}\text{Sr}_{0.2}\text{Ni}_{0.4}\text{Cu}_{0.6}\text{O}_{4+\delta}/\text{GDC}$	640	2.12	*	[28]
$\text{Nd}_{1.90}\text{Sr}_{0.1}\text{Ni}_{0.9}\text{Co}_{0.1}\text{O}_{4+\delta}/\text{GDC}$	700	0.69	0.88	This work
$\text{Nd}_{1.6}\text{Sr}_{0.4}\text{NiO}_4/\text{GDC}$	700	0.84	*	[30]
$\text{Nd}_{1.8}\text{Sr}_{0.2}\text{NiO}_4/\text{GDC}$	700	0.93	1.39	[29]
$\text{Nd}_{1.4}\text{Sr}_{0.6}\text{NiO}_4/\text{GDC}$			0.98	[22]
$\text{Nd}_{1.2}\text{Sr}_{0.8}\text{NiO}_4/\text{GDC}$			0.93	[22]
$\text{Nd}_{2}\text{NiO}_4/\text{GDC}$			1.26	[6]
$\text{Nd}_{1.8}\text{Sr}_{0.2}\text{Ni}_{0.6}\text{Cu}_{0.4}\text{O}_{4+\delta}/\text{GDC}$			1.31	[29]
$\text{Nd}_{1.8}\text{Sr}_{0.2}\text{Ni}_{0.4}\text{Cu}_{0.6}\text{O}_{4+\delta}/\text{GDC}$			1.34	[29]

Electrochemical characterization of NSNCO01

The amplitude test allowed knowing the regions of response of the electrolyte and the electrode. For this, the temperature is set by varying the amplitude (ΔE), two temperatures are chosen, 385 and 484 °C. The Nyquist diagrams stored in the frequency range 10^6 to 10^{-2} Hz to different amplitude values, in air, are shown in Figure 5 & 6.

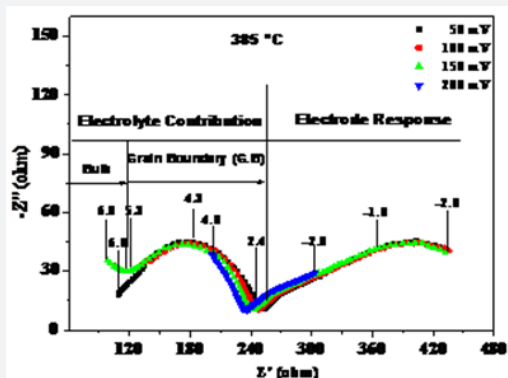


Figure 5: Impedance diagram in air for NSNCO01/GDC/NSNCO01 symmetrical cell at various amplitude and at 385 °C.

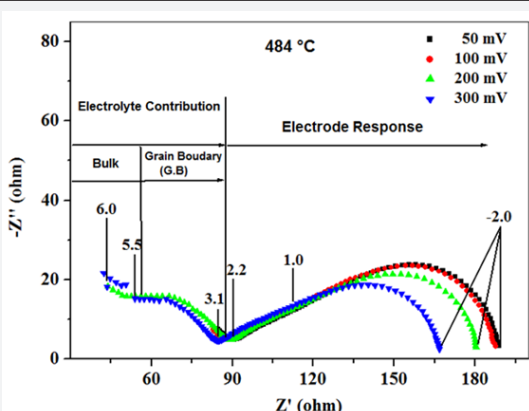


Figure 6: Impedance diagram in air for NSNCO01/GDC/NSNCO01 symmetrical cell at various amplitude and at 484 °C.

Several contributions can be distinguished. Some of them can be attributed to the GDC electrolyte (high-frequency) response, while the low frequency phenomena reflect the interface process (electrolyte / electrode) and electrode detailed as follows [27]:

At high-Frequency (HF): Two semicircles were distinguished; the first contribution, highlighted for frequencies above 10^5 Hz, corresponding to the intra-granular conduction of ions O^{2-} (contribution of "bulk"). While the second, located at frequencies between 10^5 and 10^2 Hz, relative to the conduction related to grain boundaries (intergranular conduction) of the electrolyte. It may be noted that these contributions are clearly visible at low temperatures (Figure 5), where as at high temperatures (Figure 6), it becomes difficult to distinguish.

At low frequency (BF): Two semicircles are distinguished (two contributions), the semicircle at medium frequency (MF) is relative to the ion transfer between the electrode (NSNCO01) and electrolyte (GDC), including the transfer of O^{2-} species. The semicircle at low frequency (LF) would be associated with electrochemical phenomena at the interface of cathode material / oxygen gas (adsorption-desorption, dissociation, electrode reaction). These reactions can be decomposed into the following steps (Eq.6-8).

- Adsorption: $\text{O}_2(\text{gaz}) \leftrightarrow \text{O}_2(\text{ads})$ (Eq.6)
- Dissociation: $\text{O}_2(\text{ads}) \leftrightarrow 2\text{O}$ (ads) (Eq.7)
- Reduction: $\text{O}(\text{ads}) + 2\text{e}^- \leftrightarrow \text{O}_2^-(\text{insere})$ (Eq.8)

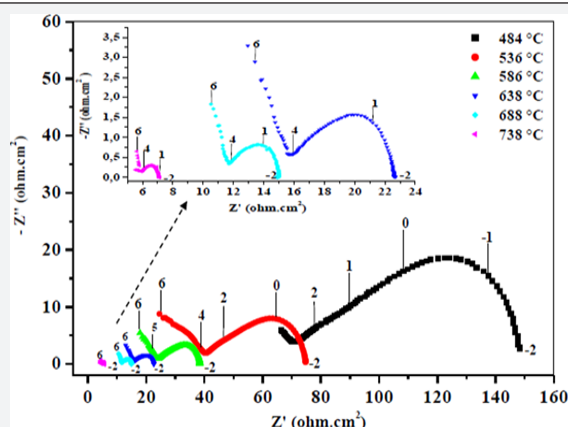


Figure 7: Nyquist plots of the $\text{Nd}_{1.9}\text{Sr}_{0.1}\text{Ni}_{0.9}\text{Co}_{0.1}\text{O}_{4+\delta}$ cathode sintered at 1000 °C for 4h and measured at different temperature in air.

The electrochemical performances of NSNCO01 were studied, the amplitude value (ΔE) was fixed at 50mV and changing the temperature, impedance spectra registered for a few values of

temperature (484-738 °C) in air, in the range of frequency 10⁶ to 10⁻²Hz were plotted and shown in Figure 7. There is a very remarkable reduction in the resistance (R_{electrolyte} and polarization resistance of electrode R_p) and therefore an increase in conductivity with increasing temperature. The kinetics of the phenomena associated with the electrodes and at the interface is thermally activated.

The electrochemical performance of the cell are measured by the following, based on resistors of different contributions to impedance measured patterns for different temperatures to 50mV (i≈0). From polarisation resistance of electrode (R_p), the surface resistance (ASR ohm.cm²) can be calculated. The Figure 8 shows the various resistances available on the impedance chart.

$$\text{ASR is calculated from the following equation: } \text{ASR} = \frac{R_p * S}{2}$$

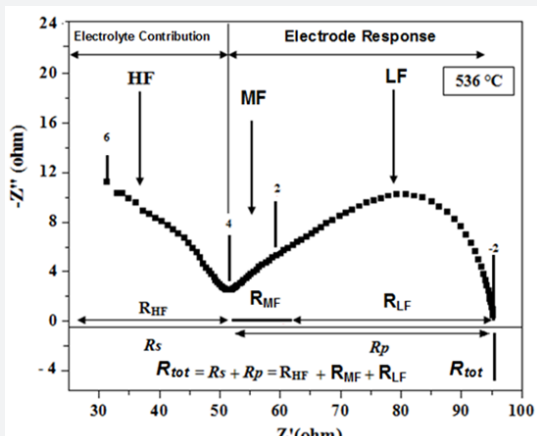


Figure 8: All resistances available on the Nyquist plot for $\text{Nd}_{1.9}\text{Sr}_{0.1}\text{Ni}_{0.9}\text{Co}_{0.1}\text{O}_{4\pm\delta}$ electrode.

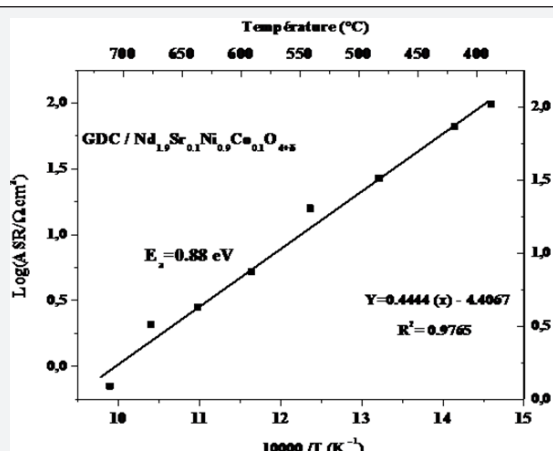


Figure 9: Temperature dependence of the polarization resistances (ASR) for $\text{Nd}_{1.9}\text{Sr}_{0.1}\text{Ni}_{0.9}\text{Co}_{0.1}\text{O}_{4\pm\delta}$ electrode measured over a temperature range of 484-738 °C in air.

Surface of cathode, R_p: The polarization resistance associated with the LF and MF contributions. Figure 9 shows the thermal variations of ASRs plotted in the Arrhenius plot. The values of ASRs and activation energy (E_a) compared to

other materials measured by other study were summarized in Table 3. Compared to all materials, the NSNCO01 electrode gave a polarization resistance (ASR) of 0.69 ($\Omega\cdot\text{cm}^2$) at 700 °C in air and gave a low activation energy of, the order 0.88eV, which indicates that $\text{Nd}_{1.9}\text{Sr}_{0.1}\text{Ni}_{0.9}\text{Co}_{0.1}\text{O}_{4\pm\delta}$ electrode is a promising cathode material for intermediate-temperature solid oxide fuel cell (IT-SOFC).

Conclusion

All of the work has to propose a new cathode material, $\text{Nd}_{1.9}\text{Sr}_{0.1}\text{Ni}_{0.9}\text{Co}_{0.1}\text{O}_{4\pm\delta}$ is a promising candidate as a cathode material for high temperature fuel cell (IT-SOFC). In the second part of this work, a electrochemical behavior carried by impedance spectroscopy at high temperature is performed on the material $\text{Nd}_{1.9}\text{Sr}_{0.1}\text{Ni}_{0.9}\text{Co}_{0.1}\text{O}_{4\pm\delta}$. Resistance of surface polarization (ASR) was evaluated at 0.69 ($\Omega\cdot\text{cm}^2$) at 700 °C which is much lower compared to ASR evaluated by some work done on other neodymium nickelates materials. In addition, the activation energy of our material is about 0.88eV, which is the lowest value compared with other materials studied to date. Which indicates that $\text{Nd}_{1.9}\text{Sr}_{0.1}\text{Ni}_{0.9}\text{Co}_{0.1}\text{O}_{4\pm\delta}$ electrode is a promising cathode material for intermediate-temperature solid oxide fuel cell (IT-SOFC).

References

1. Kharton VV, Kovalevsky AV, Avdeev M, Tsipis EV, Patrakeev MV, et al. (2007) Chemically Induced Expansion of $\text{La}_2\text{NiO}_{4\pm\delta}$ -Based Materials. *Chem Mater* 19(8): 2027-2033.
2. Boehm E, Bassat JM, Dordor P, Mauvy F, Grenier JC, et al. (2005) Solid State Ionics 2717-2725.
3. Mauvy F, Lalanne C, Bassat JM, Grenier JC, Zhao H, et al. (2005) Oxygen reduction on porous $\text{Ln}_2\text{Ni}_{04+\delta}$ Electrodes 25: 2669-2672.
4. Ferkihi M, Ahmed Yahia H (2016) Materials Research Bulletin 83: 268-274.
5. Ferkihi M, Ringueude A, Cassir M (2016) J Solid State Electrochem 20: 911-920.
6. Mauvy F, Bassat JM, Boehm E, Manaud JP, Dordor P, et al. (2003) Oxygen electrode reaction on $\text{Nd}_2\text{Ni}_{04+\delta}$ cathode materials: impedance spectroscopy study. Solid State Ionics 158: 17-28.
7. Dailly J, Fourcade S, Largeteau A, Mauvy F, Grenier JC, et al. (2010) Marrony M, *Electrochim. Acta* 55: 5847-5853.
8. Mauvy F, Lalanne C, Bassat JM, Grenier JC, Brisse A, et al. (2009) Solid State Ionics 18: 1183-1189.
9. Montenegro-Hernandez A, Vega-Castillo J, Mogni L, Caneiro A (2011) *Internat J Hydrog energ* 36: 15704-15714.
10. Soorio M, Skinner SJ (2006) Solid State Ionics 177: 2081-2086.
11. Khandale AP, Bhoga SS (2010) *J Power Sources* 195: 7974-7982.
12. Khandale AP, Bhoga SS, Kumar RV (2013) Solid State Ionics 238: 1-6.
13. Jorgensen JD, Dabrowski B, Pei S, Richards DR, Hinks HG (1989) *Physical Review* B40: 2187.
14. Vashook VV, Yushkevich II, Kokhonovsky LV, Makhanovsky LV, Makhnach LV, et al. (1999) Solid State Ionics 119: 23-30.
15. Nakamura T, Keiji Yashiro, Kazuhisa Sato, Junichiro Mizusaki (2010) Solid State Ionics 181: 402-411

16. Skinner SJ, Kilner JA (2000) Solid State Ionics 135 709-712.
17. Sun LP, Li Q, Zhao H, Huo LH, Grenier JC (2008) Journal of Power Sources 183: 43-48.
18. Ferkhi M, Khelili S, Zerroual L, Ringuede A, Cassir M, et al. (2009) Electrochimica Acta 54: 6341-6346.
19. Ferkhi M, Ringuede A, Khaled A, Zerroual L, Cassir M (2012) Electrochimica Acta 75: 80-87.
20. Vibhu V, Rougier A, Nicollet C, Flura A, Grenier JG, et al. (2015) Solide State Ionics 278.
21. Chaker H, Roisnel T, Potel M, Hassen RB (2004) Journal of Solid State Chemistry 177: 4067-4072.
22. Cheriti M, Kahoul A (2012) Materials Research Bulletin 47: 135-141.
23. Barr TL (1994) Modern ESCA, The Principles and Practice of X-Ray Photoelectron Spectroscopy, Boca Raton: CRC Press, USA.
24. Iwanowski RJ, Heinonen MH, Pracka I, Kachniarz J (2013) Appl Surf. Sci 283: 168-174.
25. Mickevicius S, Grebinskij S, Bondarenka V, Vengalis B, Sliuziene K, et al. (2006) J Alloy Compound 423: 107-111.
26. Moulder F, Stickle WF, Sobol PE, Bomben (1992) Handbook of X-ray Photoelectron Spectroscopy, by Perkin-Elmer Corporation, Physical Electronics Division.
27. Escudero MJ, Aguadero A, Alonso JA, Daza L (2007) 611: 107-116.
28. Khandale AP, Bansod MG, Bhoga SS (2015) Solid State Ionics 276: 127-135.
29. Khandale AP, Punde JD, Bhoga SS (2013) Solid State Electrochem 17: 617-626.
30. Punde JD, Khandale AP, Bhoga SS (2013) Indian Journal of Pure and Applied Physics 51: 376-380.



This work is licensed under Creative Commons Attribution 4.0 Licens
DOI: [10.19080/JOJMS.2017.02.555600](https://doi.org/10.19080/JOJMS.2017.02.555600)

**Your next submission with Juniper Publishers
will reach you the below assets**

- Quality Editorial service
- Swift Peer Review
- Reprints availability
- E-prints Service
- Manuscript Podcast for convenient understanding
- Global attainment for your research
- Manuscript accessibility in different formats
(Pdf, E-pub, Full Text, Audio)
- Unceasing customer service

Track the below URL for one-step submission

<https://juniperpublishers.com/online-submission.php>